Electrophoretic mobilities of neutral analytes and markers in aqueous solutions of Hofmeister salts

Tomáš Křížek[1], Anna Kubíčková[1], Jana Hladílková[2], Pavel Coufal[1], Jan Heyda[3*], Pavel Jungwirth[2*]

[1]Faculty of Science, Department of Analytical Chemistry, Charles University in Prague, Prague, Czech Republic

[2]Institute of Organic Chemistry and Biochemistry, Academy of Sciences of the Czech Republic, and Center for Biomolecules and Complex Molecular Systems, Prague, Czech Republic

[3]Soft Matter and Functional Materials, Helmholtz-Zentrum Berlin, Hahn-Meitner Platz 1, 14109 Berlin, Germany

Correspondence: Jan Heyda, Helmholtz-Zentrum Berlin, Hahn-Meitner Platz 1, 14109 Berlin, Germany and Pavel Jungwirth, Institute of Organic Chemistry and Biochemistry, Academy of Sciences of the Czech Republic, and Center for Biomolecules and Complex Molecular Systems, Prague, Czech Republic, Flemingovo nám. 2, 16610 Prague 6, Czech Republic

***Corresponding authors. E-mails:** jan.heyda@helmholtz-berlin.de, pavel.jungwirth@uochb.cas.cz

List of abbreviations: TUR - thiourea, DMSO - dimethylsulfoxide, NMA - N-methylacetamide, MD – molecular dynamics, I – ionic strength, g(r) – radial distribution function

Keywords: Electrophoretic markers, Ion-specific effects, Ion-specific mobilization, Molecular dynamics simulations, Neutral analytes

Total number of words: 5308

Abstract

Small neutral organic compounds have traditionally the role of markers in electrophoresis, as they are expected to have zero electrophoretic mobility in external electric fields. The background electrolyte contains, however, ions which have unequal affinities to the neutral molecules, which in turn results in their mobilization. In this study we focused on two electrophoretic markers - thiourea and dimethylsulfoxide, as well as on N-methyl acetamide as a model of the peptide bond. By means of capillary electrophoresis and all atom molecular dynamics simulations we explored mobilization of these neutral compounds in large set of Hofmeister salts. Employing a statistical mechanics approach, we were able to reproduce by simulations the experimental electrophoretic mobility coefficients. We also established the role of the chemical composition of marker and the background electrolyte on the measured electrophoretic mobility coefficient. For N-methyl acetamide, we interpreted the results in terms of the relative affinities of cations vs. anions to the peptide bond.

1 Introduction

Due to the presence of the electro-osmotic flow (EOF) [1] it is practically impossible to establish absolute electrophoretic mobilities of charged solutes. Therefore, electrophoretic mobilities are reported with respect to neutral markers [2]. Within this procedure, it is tacitly assumed that such a marker follows the EOF, providing thus a solid reference for evaluating solute mobilities. However, if ions are present in the background electrolyte, it is not a priori clear why the marker should move exactly with the velocity of the EOF.

Background electrolytes (BGE) are known to affect electrophoretic mobilities [3-5]. An extreme example of the effect of electrolyte ions is overcharging [6]. A highly charged solute can induce condensation of multivalent ions from the solution, which then effectively leads to the reversal of its electrophoretic mobility [7]. For neutral markers, such a dramatic effect like overcharging cannot, in principle, occur. Nevertheless, if cations and anions from the electrolyte exhibit different affinities for the marker, this leads to its non-zero electrophoretic mobility, which is marker- and electrolyte-specific. In this study, we demonstrate by capillary electrophoresis that two common markers, thiourea (TUR) and dimethyl sulfoxide (DMSO), have indeed different electrophoretic mobilities, and provide a detailed interpretation of this effect using atomistic molecular dynamics (MD) simulations. In this context we stress that in the present work we focus on atomistic details behind the electrophoretic mobilization rather than on multiscale approaches toward simulation at the continuum BGE level [8].

A non-vanishing mobility of neutral solutes in BGE is not necessarily limited to electrophoretic markers. Any neutral molecule can exhibit such a behavior and the strength of the effect depends on the relative affinities of electrolyte cations vs. anions for the solute. These in turn are functions of the detailed chemical composition of the solute, as well as the chemical specificity BGE. This specificity is usually expressed in the Hofmeister series, which originally ordered ions according to their ability to salt out proteins. In this respect it is also worth investigating how the Hofmeister ions interact with

the amide group forming the peptide bond in proteins. N-methyl acetamide (NMA) is a small neutral solute which is often employed as a simple model for the peptide bond [9-12]. Here, we establish the electrophoretic mobility of the neutral NMA molecule by capillary electrophoresis and MD simulations, and compare it to results for the thiourea and DMSO markers.

Our study aims at weaker ion-neutral particle interactions compared to those which are present for complexation agents, such as functionalized cyclodextrines, or crown ethers. The strength of complexation agents stems predominantly from their optimized shape, which results in multiple binding. On the weaker binding side, a very weak ion-specific affinity for alkali and alkali-earth metal ions to zwitterionic buffer TAPS was reported [13]. Older evidence, albeit only qualitative, was presented for ion-specific affinity to polar polymethacrylamide polymer exhibiting a mobilization effect, which depend on the nature of cations and anions [14]. Most recently, it has been pointed out that the values of complexation constants for an analyte-complexation agent pair are indeed substantially affected by the type and concentration of buffer constituents [15-17]. Here, we address these issues experimentally and computationally with considerable detail.

2 Material and methods

2.1 Chemicals

All chemicals used to prepare background electrolytes were purchased in p.a. purity, thiourea and DMSO were purchased from Merck (Germany), and NMA from Sigma-Aldrich (USA). Background electrolytes (BGEs) and samples were prepared using deionized water produced by a Milli-Q system, Millipore (USA). BGEs were prepared by mixing two solutions of equal ionic strength in the v/v ratio 4/1; an aqueous solution of appropriate sodium or acetate salt and aqueous acetate buffer, pH 5.5 (adjusted by NaOH).

2.2 Instrumentation

Experiments were performed at a 7100 CE instrument, Agilent Technologies (Germany), in combination with diode array UV detector. Absorbance signals at 200, 214 and 254 nm were collected. Signal at 200 nm was used for data evaluation. The 214 and 254 nm signals were used to confirm the identity of analytes based on differences in their UV spectra. Temperature of capillary cassette was maintained at 25 °C using an air-cooling system.

2.3 Mobility measurements

A non-coated fused silica capillary, 75 μm id, was purchased from Caco (Slovakia) and cut to 80.0 cm total length (71.5 cm to the detection window). Prior to each run, the capillary was flushed 5 min with 1 M NaOH, 5 min with deionized water and 2 min with BGE using a pressure of 100 kPa. Sample was composed of BGE with addition of NMA and an EOF marker (TUR, DMSO, or both). Concentrations in the injected sample were as follows: 10.0 mmol/L NMA, 1.3 mmol/L TUR and 2.8 mmol/L DMSO. Sample was injected into the capillary using a pressure of 5 kPa for 3 s. Subsequently, a voltage of +15 kV was applied for 15 min. Then vials with BGE were replaced with fresh ones and voltage was reapplied for another 15 min. This procedure was repeated four times so that the total time of voltage application was 60 min. During this period, components of the sample were carried by electroosmotic flow and their electrophoretic mobility. At the final stage of the experiment, zone of aqueous solution of the marker (TUR or DMSO) was injected with a pressure of 5 kPa for 3 s. Finally, all the zones were mobilized by the application of 5 kPa of pressure and the UV detector recorded the zones passing through the detection window. The time had been measured and the UV signal collected since the voltage was applied for the first time (t=0). The relative electrophoretic mobility was calculated using the equation (1, see below).

2.4 All-atom MD simulation

MD simulations of single solute, NMA[18], thiourea or DMSO in salt solution were performed with Gromacs 4.5.3 simulation package [19]. In order to obtain converged radial distribution functions for ions and solute, 100 ns simulation runs with 2 fs time step and 1 ps sampling frequency were performed. Temperature and pressure at ambient conditions (300 K and 1 atm) were controlled by weak velocity rescale coupling scheme [20], and Parinello-Rahmann barostat [21] respectively. To avoid finite size effects in solution structure, we studied large system with a size of 50Åx50Åx50Å, where single solute was immersed in 5000 SPC/E water molecules [22] and 120 (60 in case of Na_2SO_4) molecules of salt (ion pairs). Namely we investigated the effect of sodium salts Na_2SO_4, CH_3COONa, NaF, NaCl, NaI, $NaClO_4$, NaSCN, CH_3SO_3Na [23-26] and acetates LiAc, NaAc, KAc, and CsAc [27]. The salt concentration was ≈1.3 M (0.65 M in case of Na_2SO_4), in order to achieve reasonable sampling of ion-distribution around solute. All simulations were performed with nonpolarizable force field, however, in case of sodium sulfate, the implicit polarizability was applied via so called charge scaling concept [28]. For methylsulfonate, thiourea and DMSO the generalized amber force field (GAFF) [29] was used, together with recommended RESP [18, 30] partial charges calculated with 6-31G* basis set at Hartree-Fock level of theory using the Gaussian program [31].

2.5 Mobility calculations

2.5.1 Experiment

We applied an experimental protocol, in which at time t=0 sample with marker and NMA was injected in and the second marker zone was injected in at the end of the experiment (i.e. when the applied electric field was turned off). We have calculated the relative electrophoretic mobility coefficient, $\Delta\mu_{salt}^{S}$, of a solute, *S*, with respect to the neutral marker, *M*, via equation 1; through times, when the solute (t_S), marker (t_M) and the second zone of marker (t_{M2}) passed the detector at the distance l_d under the electric field U/l_c applied for the time t_U.

$$\Delta\mu_{salt}^{S} = \mu_{salt}^{S} - \mu_{salt}^{M} = \frac{(t_M - t_S)l_d}{(t_{M2} - t_S)l_U} \cdot \frac{l_c}{U} \quad (1)$$

In the equation above, solute *S* stays for NMA, marker *M* for thiourea, or DMSO, and *salt* assign sodium (NaF, … , NaSCN) or acetate salts (LiAc, …, $CaAc_2$) resp. Please note that μ_{salt}^{S} and μ_{salt}^{M} are absolute electrophoretic mobilities (without any reference), as could be determined if the electroosmotic flow is exactly known or entirely suppressed.

Most of the salts that were investigated in this study were strong electrolytes. Therefore sodium acetate buffer of the same ionic strength (mixed with v/v ratio 4/1) was added. To recover the mobility caused by neat salt solution, we assumed the simple additivity of salt effects on solute.

$$\mu_{salt}^{S} = \frac{1}{4}\left(5 \cdot \mu_{\frac{salt}{NaAc}}^{S} - 1 \cdot \mu_{NaAc}^{S}\right) for\ 1{:}1\ salts\ (2a)$$

$$\mu_{salt}^{S} = \frac{3}{4}\left(5 \cdot \mu_{\frac{salt}{NaAc}}^{S} - 1 \cdot \mu_{NaAc}^{S}\right) for\ 2{:}1\ salts\ (2b)$$

2.5.2 Simulation

Following our recent publication [7, 32], we neglected the hydrodynamic interactions of the solute and assume it to be spherical. With that in mind, we can apply the formula (equation 3) for absolute electrophoretic mobility in solution, μ_{salt}^{S}, as introduced by Friedman and Altenberger [33].

$$\mu_{salt}^{S}(c_{salt}) = \mu_{lim}^{S} + \frac{2}{3}\frac{e}{\eta}\sum_{i=X^+,Y^-} z_i c_{salt} \int_0^\infty (g_{Si}(r) - 1) r \mathrm{d}r \quad (3)$$

Grounded in ion-solute radial distribution functions $g_{Si}(r)$, the absolute electrophoretic mobility coefficient μ_{salt}^{S}, for solute, *S*, in salt solution (or salt mixture, with ions X^+, Y^-) with concentration, ρ_i, of ionic species with charge, z_i, can be determined. In the equation 3, *e* stays for the elementary charge and η for the water viscosity coefficient. For the neutral solute, the mobility in neat water (i.e.

in the absence of salt) vanishes, $\mu_{lim}^{S} = 0$ and the relative electrophoretic mobility is simply

$\Delta\mu_{salt}^{S}(\varrho_i) = \mu_{salt}^{S}(\varrho_i) - \mu_{salt}^{M}(\varrho_i)$.

3 Results

In our recent studies [32, 34, 35], we were able to quantify ion-specific effects on charged peptides. Further research for ion-specific effects led us to perform apparently hopeless CE experiment, where the mixture of neutral, but polar molecules, NMA, DMSO, and thiourea in sodium methylsulfonate / sodium acetate BGE was subject to electric field. The result is present in Figure 1 and the clear separation was achieved. This is clear evidence that the different affinity of sodium and methylsulfonate to these molecules lead to measurable and distinguishable mobilization.

The ion-specificity is responsible for this mobilization; therefore we followed the same protocol with number of sodium and acetate salts spanning the whole broadness of Hofmeister series. Relative electrophoretic mobility coefficients for NMA, DMSO and thiourea in salt solutions with ionic strength I=250mM are summarized in Table 1. Surprisingly the traditional electrophoretic markers thiourea and DMSO are separated in all solutions. The mobility difference is about 0.4 e.u., and is positive (DMSO travels more as cation then thiourea) in all salts except of sodium perchlorate, where it is negative. This is merely experimental evidence; indeed, the interpretation of these striking results based on CE measurements only is unclear.

In order to shed more light into this complex problem, we performed MD simulations for all salt solutions, for which reliable parameters were available. Due to sampling issues, we were able to perform simulations at salt concentration of ~1M. According to Equation 3, the connection of local solution structures (in terms of radial distribution functions) with electrophoretic mobility coefficient scales predominantly linearly with salt concentration. Therefore we did not compare the electrophoretic mobilities, but their slopes, $\Delta\mu$ / Δc_{salt} (mobility change per molar concentration of added salt), which is approximately constant in concentration range investigated here.

Concentration dependence of relative electrophoretic mobilities is presented in Figure 2, where we see clear separation of NMA from thiourea. For acetate salts, we see that Ca^{2+}, Mg^{2+}, and Li^{+} mobilize NMA in positive direction compared to thiourea, while Cs^{+} in negative direction, as summarized in the left part of Table 2. Addition of sodium acetate does not lead to separation. For sodium salts, SO_4^{2-}, F^{-}, Cl^{-}, $CH_3SO_3^{-}$ mobilize NMA in positive direction, while ClO_4^{-} in negative direction compared to thiourea. Once measurable, we see fairly well linear growth with salt concentration. As all experiments are performed in sodium acetate buffer, we assumed simple additive behavior (Equation 2) and calculated contribution of each salt to the mobilization as presented in left part of Table 3.

The representative subset of MD results are shown in Figure 3 and 4 where we present 3 acetate salts (Li^{+}, Na^{+}, Cs^{+}) and 3 sodium salts (Ac^{-}, Cl^{-}, ClO_4^{-}) for clarity. Results for DMSO and for complete set of salts are provided in the Supporting Information. First we determined the radial distribution functions for ions around NMA, thiourea, and DMSO which represent their radially resolved excess or depletion. Following the Equation 3, we subsequently determined the absolute electrophoretic mobility coefficient μ (mobility in absolute reference frame).

For example, let us compare the radial distribution of Li^{+} and Cs^{+} around NMA. We see that while Li^{+} is modestly in excess next to NMA and then reaches bulk density, Cs^{+} is purely depleted in the vicinity of NMA before it reaches bulk density. This means that around NMA in Li^{+}, there is more positive charge compared to the situation in Cs^{+}**.** Electrophoretic mobility in LiAc is virtually zero, so the action of Li^{+} and Ac^{-} compensates, while in CsAc it is negative (2 e.u. per 1M of added salt) meaning that there is more acetate anions around compared to cesium cations. The difference in electrophoretic mobility coefficient of NMA in LiAc and in CsAc can be assigned to their different affinity to NMA and NMA vicinity. We should note that this mechanistic description is evident for local affinity; however the average over many layers and correlated contribution from counterion is far less intuitive. The counterion effects were small in the set of investigated salts, which simplifies

the interpretation the g(r) and μ(r) relation, and are provided in the Supporting Information for completeness.

Due to significant differences in structure, polarity, hydrogen-bonding capability of NMA and thiourea, it is not surprising that the affinity of cations vary. Still, the same spirit as described above for LiAc and CsAc can be applied to understand the direction and magnitude of analyte mobilization.

Slopes for relative electrophoretic mobility coefficients $\Delta\mu / \Delta c_{salt}$ are provided in the right part of Tables 2 and 3. At first glance, theory is in accord with experiment. Salts which lead to faster mobilization in cationic direction of NMA (LiAc, NaF, or sodium methylsulfonate), or thiourea (CsAc, or $NaClO_4$) respectively are correctly proposed. Overall we obtained good quantitative agreement in electrophoretic mobility coefficients; particularly sound are the results for acetate salts (Li^+, Na^+, Cs^+). The reasons for deviation for sodium chloride and sodium sulphate will be discussed in the next section.

Before we take a step to discussion, it is beneficial to realize that the radial distribution function describes well spherical and homogeneous objects. However, NMA, thiourea, and DMSO are far from being spherical and their surface possesses polar (even with opportunities for H-bonding) and nonpolar patches. Therefore in Figure 5, we present the ion affinity in terms of spatial distribution functions (at level of 2-3 x the bulk density). We can clearly see the position and magnitude of the affinity of ions, which results (after averaging) in roughed g(r)-description in Figure 3 and 4. The colours of ions in Figure 4 and 5 are consistent for clarity. The difference affinity towards surface of NMA between soft perchlorate and hard acetate is evident.

4 Discussion

Experimental results presented in Table 1 clearly demonstrate that the DMSO and thiourea markers get separated from each other in all investigated BGE. For any analyte the measured mobility is thus only of a relative value, as determined with respect to particular marker. This issue becomes critical when electrophoretic mobilities are small, such as for neutral analytes, and when changes in mobilities are converted into physico-chemical properties like binding or association constants.

In this respect the insight gained via parallel MD simulations is invaluable, as the solute mobilization in an absolute reference frame is directly obtained together with individual contributions from cationic and anionic affinities (Table S4, and Figures 3, 4, S5, S6). Thanks to the fact that an underlying theory is available [8, 33], we can then rationalize measurable mobility coefficients in terms of the microscopic structure of the solution next to the neutral solute. We can thus translate the excess or depletion of ions (or equally the charge in the ionic atmosphere) in the nearest several layers of the solvent around the solute into the resulting electrophoretic mobility.

Clearly, the chemical structure and composition (for details see Table S1) of electrophoretic markers, with partially hydrophobic and partially polar surfaces, is the key factor behind the complex and nonlinear action of salts. Hofmeister ordering for single surface type is often observed for salt ions [36], however, already for short oligopetides the action of salts can be reversed by changing their functional groups [34, 37]. This raises a question, whether an ideal marker, which would move with the EOF in every salt solution, could exist at all. For each marker it should be possible to find a salt, in which it is essentially immobile. However, based on the above observations on ion specificity, finding a marker which is immobile in many different salt solutions is very unlikely. And ideal neutral marker in this respect would be one that behaves exactly like the solvent, i.e., tritiated water, which is, however, not a practical choice.

Most results obtained in present simulations agree with previously observed behaviour of Hofmeister ions. For example, the large and only weakly polar carbonothioyl group in thiourea binds

large cations rather than smaller ones, in contrast to the smaller and more polar carbonyl group in NMA and sulfinyl group in DMSO (Figures 3 and S1). Most complex in this respect is the action of sodium perchlorate, which is known to be strongly bound to both polar and nonpolar regions of the solute.

From the computational side, we focused mainly on monovalent ions, since weak interactions of these ions with neutral solutes and with each other lead to a near-linear behaviour in which CE and MD performed at different BGE concentrations can be directly compared. Polyvalent ions were mostly avoided also due to well-known deficiencies of their force fields. The only exception was Na_2SO_4 for which we employed our recently refined parameterization of sulphate implicitly accounting also for polarization effects. However, due to relatively high salt concentration, the ion affinities to NMA and thiourea are unlikely to grow linearly with Na_2SO_4 concentration. This together with low activity of the Na_2SO_4 solution explains the observed disagreement between CE and MD results in this case.

Results for sodium halide salts are worth an additional remark. We can see from Figure S2 and Table S4 that present the anionic affinities and mobilization of NMA, that fluoride is repelled, chloride is neutral, and iodide is attracted to NMA surface, in agreement with previously published data [10, 11]. An opposite anionic trend is expected (and indeed observed) for thiourea, since the H-bonding power follows the reversed ordering $F^- > Cl^- > I^-$. Although qualitatively captured, the proper quantitative balance was not reached for chloride anion as documented by the inaccurate prediction of the relative electrophoretic mobility $\Delta\mu_{NaCl}^{NMA/TUR}$.

5 Concluding remarks

The principle novelty of the present study lies in a combined application of CE with MD simulations to electrophoretic mobilities of neutral markers and solutes, allowing on one hand for verification of the simulations by the electrophoretic technique and, on the other hand, for rationalization of the measured effects via a computational description at an atomistic level. We have thus demonstrated

that CE has sufficient resolution to allow us to study and quantify subtle ion-specific effects on electrophoretic mobilities of neutral markers and analytes. As a result, we show that neutral markers and solutes do not move with the EOF, but exhibit non-vanishing solute- and BGE-specific electrophoretic mobilities.

Our results also provide a fresh look at the protein-ligand binding data, as well as stability constants, which have been determined within the family of methods of affinity electrophoresis and similar techniques [38-40]. There has been a debate [9], how good NMA, as the present model for the peptide bond, represents the properties of the connecting unit of the protein backbone. Other model compounds were proposed, among which elastine like polypeptides and oligoglycines could be potential targets of a future combined CE and MD study [11, 34, 37].

In the future, our work could also prove useful in the new field of electrophoretic NMR (eNMR)[41, 42], which aims at quantification of the binding of small charged molecules to weakly charged or neutral proteins. Due to the presence of BGE, the nonspecific electrostatic effects (counterion condensation being an extreme case), as well as salt specific effects, must be properly treated in order to reach correct quantitative conclusions. In this context, it is worth stressing that CE probes in the intermediate *r*-dependent interaction length-scale (see equation 3), compared on one side to the more local r^{-4}-dependent regime of NMR *[43, 44]* or similarly short range IR [45] and, on the other side, to the long range r^{2}-dependent thermodynamic regime [46].

Supplementary Information: Results for large set of sodium and acetate salts are provided, which supplement the figures in main text. Specifically, the spatial and radial distribution functions are presented in terms of figures and ion contributions to mobility coefficients in terms of tables.

6 Acknowledgements

A. K., T. K., and P. C. acknowledge SVV project from the Charles University and research project MSM0021620857 of the Ministry of Education, Youth and Sports for funding. P. J. acknowledges the Czech Science Foundation (grant no. P208/12/G016) for support and thanks the Academy of Sciences for the Praemium Academie award. J.He. acknowledge funding from the Alexander-von-Humboldt (AvH) Stiftung, Germany. J. Hl. thanks the IMPRS in Dresden for support.

The authors declare no conflict of interest.

7 References

[1] Ghosal, S., *Electrophoresis* 2004, *25*, 214-228.

[2] Williams, B. A., Vigh, C., *Anal. Chem.* 1996, *68*, 1174-1180.

[3] Ibrahim, A., Allison, S. A., Cottet, H., *Anal. Chem.* 2012, *84*, 9422-9430.

[4] Koval, D. A., Kasicka, V., Zuskova, I., *Electrophoresis* 2005, *26*, 3221.

[5] Pitts, E., *Proc. R. Soc. London, Ser. A* 1953, *217*, 43.

[6] Lyklema, J., *Colloids Surf., A* 2006, *291*, 3-12.

[7] Kubickova, A., Krizek, T., Coufal, P., Vazdar, M., *et al.*, *Phys. Rev. Lett.* 2012, *108*.

[8] Rotenberg, B., Pagonabarraga, I., *Mol. Phys.* 2013, *111*, 827-842.

[9] Bolen, D. W., Rose, G. D., *Annu. Rev. Biochem.* 2008, pp. 339-362.

[10] Heyda, J., Vincent, J. C., Tobias, D. J., Dzubiella, J., Jungwirth, P., *J. Phys. Chem. B* 2010, *114*, 1213-1220.

[11] Nandi, P. K., Robinson, D. R., *J. Am. Chem. Soc.* 1972, *94*, 1299-&.

[12] Schrier, E. E., Schrier, E. B., *J. Phys. Chem.* 1967, *71*, 1851-&.

[13] Muzikář, M., Havel, J., Macka, M., *Electrophoresis* 2002, *23*, 1796-1802.

[14] Chatterjee, S. K., Prokopová, E., Bohdanecký, M., *Eur. Polym. J.* 1978, *14*, 665 - 670.

[15] Beneš, M., Riesová, M., Svobodová, J., Tesařová, E., *et al.*, *Anal. Chem.* 2013, *85*, 8526-8534.

[16] Müllerová, L., Dubský, P., Svobodová, J., Gaš, B., *Electrophoresis* 2013, *34*, 768-776.

[17] Riesová, M., Svobodová, J., Tošner, Z., Beneš, M., *et al.*, *Anal. Chem.* 2013, *85*, 8518-8525.

[18] Wang, J. M., Cieplak, P., Kollman, P. A., *J. Comput. Chem.* 2000, *21*, 1049-1074.

[19] Van der Spoel, D., Lindahl, E., Hess, B., Groenhof, G., *et al.*, *J. Comput. Chem.* 2005, *26*, 1701-1718.

[20] Bussi, G., Donadio, D., Parrinello, M., *J. Chem. Phys.* 2007, *126*.

[21] Parrinello, M., Rahman, A., *J. Appl. Phys.* 1981, *52*, 7182-7190.

[22] Berendsen, H. J. C., Grigera, J. R., Straatsma, T. P., *J. Phys. Chem.* 1987, *91*, 6269-6271.

[23] Rajamani, S., Ghosh, T., Garde, S., *J. Chem. Phys.* 2004, *120*, 4457-4466.

[24] Jungwirth, P., Tobias, D. J., *J. Phys. Chem. B* 2001, *105*, 10468-10472.

[25] Jagoda-Cwiklik, B., Vácha, R., Lund, M., Srebro, M., Jungwirth, P., *J. Phys. Chem. B* 2007, *111*, 14077-14079.

[26] Wick, C. D., Dang, L. X., Jungwirth, P., *J. Chem. Phys.* 2006, *125*, 024706.

[27] Hess, B., van der Vegt, N. F. A., *Proc. Natl. Acad. Sci. U. S. A.* 2009, *106*, 13296-13300.

[28] Leontyev, I. V., Stuchebrukhov, A. A., *J. Chem. Theory Comput.* 2010, *6*, 3153-3161.

[29] Wang, J. M., Wolf, R. M., Caldwell, J. W., Kollman, P. A., Case, D. A., *J. Comput. Chem.* 2004, *25*, 1157-1174.

[30] Duan, Y., Wu, C., Chowdhury, S., Lee, M. C., *et al.*, *J. Comput. Chem.* 2003, *24*, 1999-2012.

[31] Frisch, M. J., Trucks, G. W., Schlegel, H. B., Scuseria, G. E., *et al.*, *Gaussian 09, Revision B.01, Gaussian, Inc., Wallingford CT*, Wallingford CT 2009.

[32] Wernersson, E., Heyda, J., Kubickova, A., Krizek, T., *et al.*, *Electrophoresis* 2012, *33*, 981-989.

[33] Altenberger, A. R., Friedman, H. L., *J. Chem. Phys.* 1983, *78*, 4162-4173.

[34] Rembert, K. B., Paterova, J., Heyda, J., Hilty, C., *et al.*, *J. Am. Chem. Soc.* 2012, *134*, 10039-10046.

[35] Wernersson, E., Heyda, J., Kubickova, A., Krizek, T., *et al.*, *J. Phys. Chem. B* 2010, *114*, 11934-11941.

[36] Schwierz, N., Horinek, D., Netz, R. R., *Langmuir* 2013, *29*, 2602-2614.

[37] Paterova, J., Rembert, K. B., Heyda, J., Kurra, Y., *et al.*, *J. Phys. Chem. B* 2013, *117*, 8150-8158.

[38] Colton, I. J., Carbeck, J. D., Rao, J., Whitesides, G. M., *Electrophoresis* 1998, *19*, 367-382.

[39] Chu, Y.-H., Avila, L. Z., Gao, J., Whitesides, G. M., *Acc. Chem. Res.* 1995, *28*, 461-468.

[40] Takeo, K., *Electrophoresis* 1984, *5*, 187-195.

[41] Griffiths, P. C., Paul, A., Hirst, N., *Chem. Soc. Rev.* 2006, *35*, 134-145.

[42] Hallberg, F., Weise, C. F., Yushmanov, P. V., Pettersson, E. T., *et al.*, *J. Am. Chem. Soc.* 2008, *130*, 7550-7551.

[43] Dengler, S., Klaus, A., Tiddy, G. J. T., Kunz, W., *Faraday Discuss.* 2012, *160*, 121-133.

[44] Holz, M., Grunder, R., Sacco, A., Meleleo, A., *J. Chem. Soc., Faraday Trans.* 1993, *89*, 1215-1222.

[45] Okur, H. I., Kherb, J., Cremer, P. S., *J. Am. Chem. Soc.* 2013, *135*, 5062-5067.

[46] Kirkwood, J. G., Buff, F. P., *J. Chem. Phys.* 1951, *19*, 774-777.

8 Tables and Table Captions:

Table 1: Quantitative separation of NMA, DMSO, and thiourea mixture in solutions of sodium salts (I = 250 mM), buffered with sodium acetate (v/v ratio 4/1). The 15 kV voltage was applied for 60 minutes and the relative electrophoretic coefficient (in 1 e.u. = $10^{-9} \cdot m^2 \cdot V^{-1} \cdot s^{-1}$) was measured.

salt	$\Delta\mu_{salt/NaAc}^{DMSO,NMA}$	$\Delta\mu_{salt/NaAc}^{DMSO,TUR}$
CH_3COONa	0.30	0.30
$NaClO_4$	-0.19	-0.44
CH_3SO_3Na	0.24	0.45
$NaSO_4$	0.25	1.20
NaF	0.00	0.22
NaCl	0.17	0.41

Table 2: Relative electrophoretic mobility of NMA with respect to thiourea as measured in acetate salts and compared with results from MD simulations. As the theoretical formula for evaluation of mobility coefficient is (in 1st order) linear in salt concentration, and theory and experiment are performed at different salt concentrations, the slope $d\Delta\mu/dc$ is compared. The experimental and theoretical values are based on results in Figures 2 and 3 resp. More detailed table with calculated absolute electrophoretic mobilities is provided in SI (Table S4).

	$d\Delta\mu_{XAc}^{NMA,TUR}/dc_{XAc}$ $[10^{-9}\cdot m^2\cdot V^{-1}\cdot s^{-1}\cdot mol^{-1}\cdot l]$	
salt	**experiment**	**simulation**
CsAc	-1.6	-1.0
KAc	---	-1.0
NaAc	0.0	0.1
LiAc	1.5	1.5
$MgAc_2$	1.0	---
$CaAc_2$	1.2	---

Table 3: Relative electrophoretic mobility of NMA with respect to thiourea as measured in sodium salts (NaX) and compared with results from MD simulations. As the theoretical formula for evaluation of mobility coefficient is (in 1st order) linear in salt concentration, and theory and experiment are performed at different salt concentrations, the slope $d\Delta\mu/dc$ is compared. The experimental and theoretical values are based on results in Figures 2 and 4 resp. The original experimental results in 4/1 NaX/NaAc buffered salt solution are provided in SI – Table S3. More detailed table with calculated absolute electrophoretic mobilities is provided in SI (Table S4).

	$d\Delta\mu_{NaX}^{NMA,TUR}/dc_{NaX}$ $[10^{-9}\cdot m^2\cdot V^{-1}\cdot s^{-1}\cdot mol^{-1}\cdot l]$	
salt	**experiment**	**simulation**
Na_2SO_4	5.0	0.1
CH_3COONa	0.0	0.1
NaF	2.0	1.3
NaCl	1.5	-1.1
CH_3SO_3Na	1.0	1.2
$NaClO_4$	-1.1	-1.4
NaI	---	-2.9
NaSCN	---	-0.6

9 Figures and Figure Captions:

Figure 1: Final electropherogram from the separation of **NMA/DMSO/Thiourea** mixture of 'analytes' in the solution of **$NaCH_3SO_3$/ CH_3COONa** 4:1, at the total ionic strength I = 250 mM, and applied voltage of + 15 kV. The UV spectra at 200 nm, 214 nm, and 254 nm in the detector show clear separation of analytes at the experimental time ~ 55 minutes. Electrophoretic mobility coefficients were determined from these electropherograms and are summarized in Table 1.

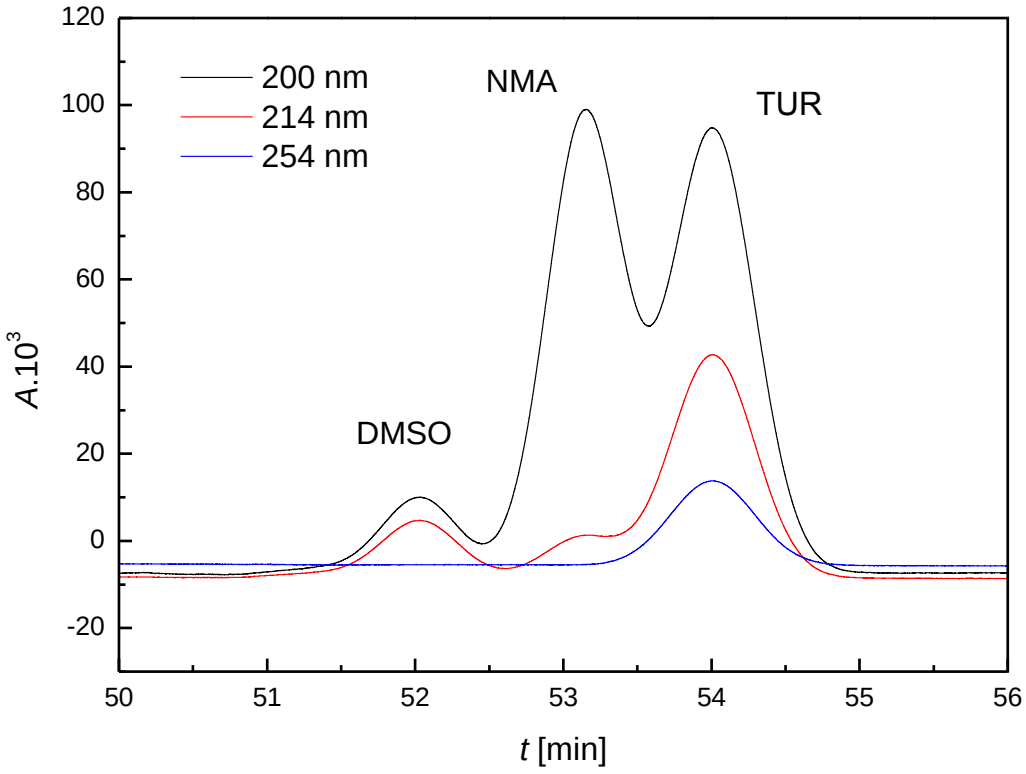

Figure 2: Measured relative electrophoretic mobilities of NMA in various acetate salts (top) and in various sodium salts (bottom) with respect to the thiourea marker. Increase of mobility per unit salt concentration is summarized in Table 2 and 3 and was calculated as the best linear fit of experimental data, and satisfying zero mobility in the absence of salt. [1e.u. = 10^{-9} $m^2V^{-1}s^{-1}$]

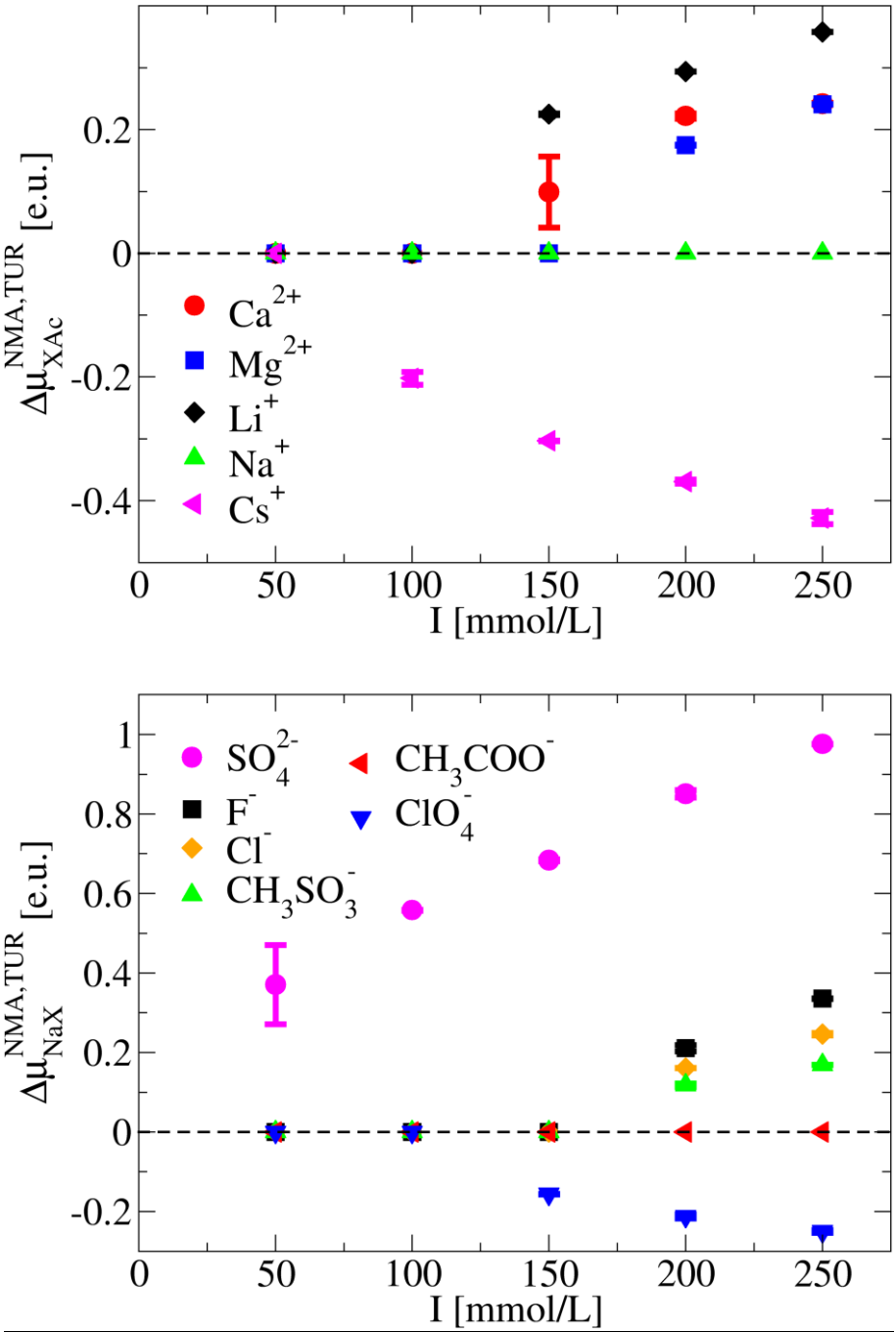

Figure 3: Structural properties of selected acetate salts (Li^+/LiAc - black, Na^+/NaAc – green, Cs^+/CsAc - pink) are presented in terms of cation-solute radial distribution functions (top panel). Thereafter calculated electrophoretic mobilities (according to equation 3) are presented in bottom panel. Results for NMA are present on the left and for thiourea on the right. Full list of salts is presented in SI. The mobility coefficients as extracted from the brown region are summarized in Table S4 and the difference in mobilities of NMA and thiourea in Table 2.

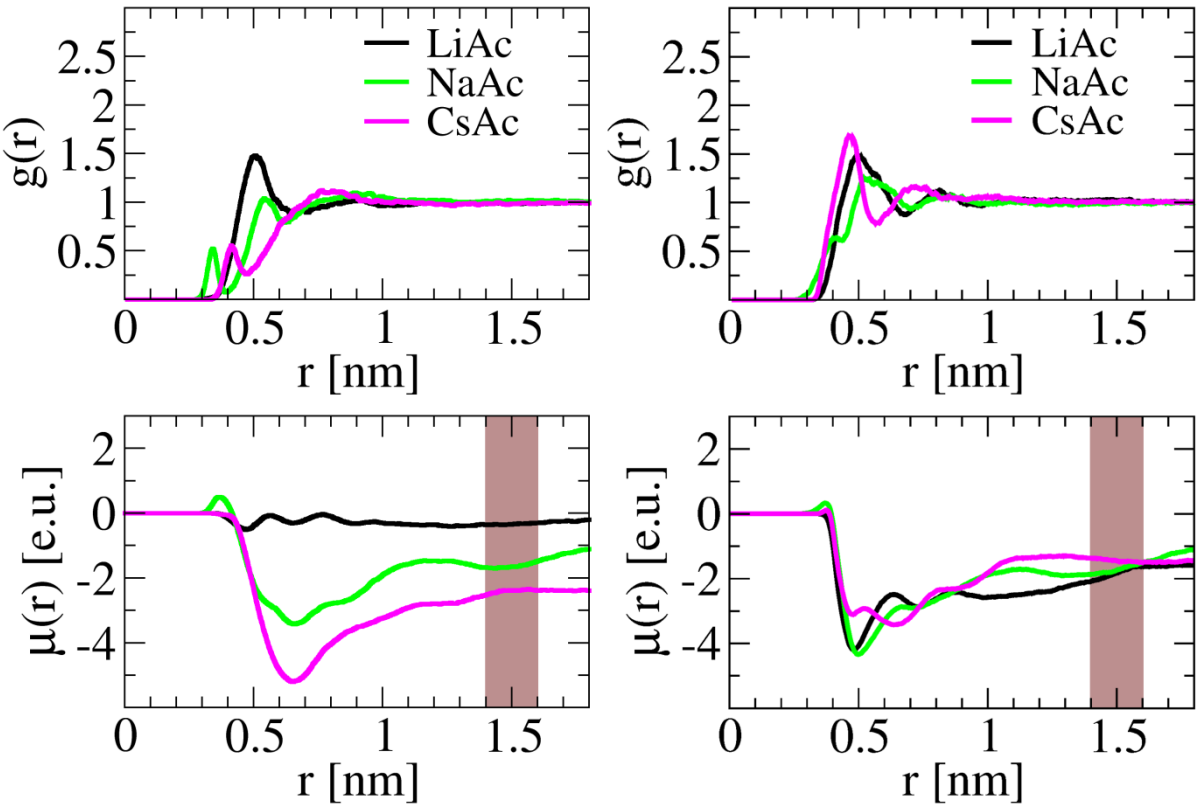

Figure 4: Structural properties of selected sodium salts (Ac^-/NaAc - red, Cl^-/NaCl – orange, ClO_4^- /$NaClO_4$ - blue) are presented in terms of anion-solute radial distribution functions (top panel). Thereafter calculated electrophoretic mobilities (according to equation 3) are presented in bottom panel. Results for NMA are present on the left and for thiourea on the right. Full list of salts is presented in the Supporting Information. The mobility coefficients as extracted from the brown region are summarized in Table S4 and the difference in mobilities of NMA and thiourea in Table 3.

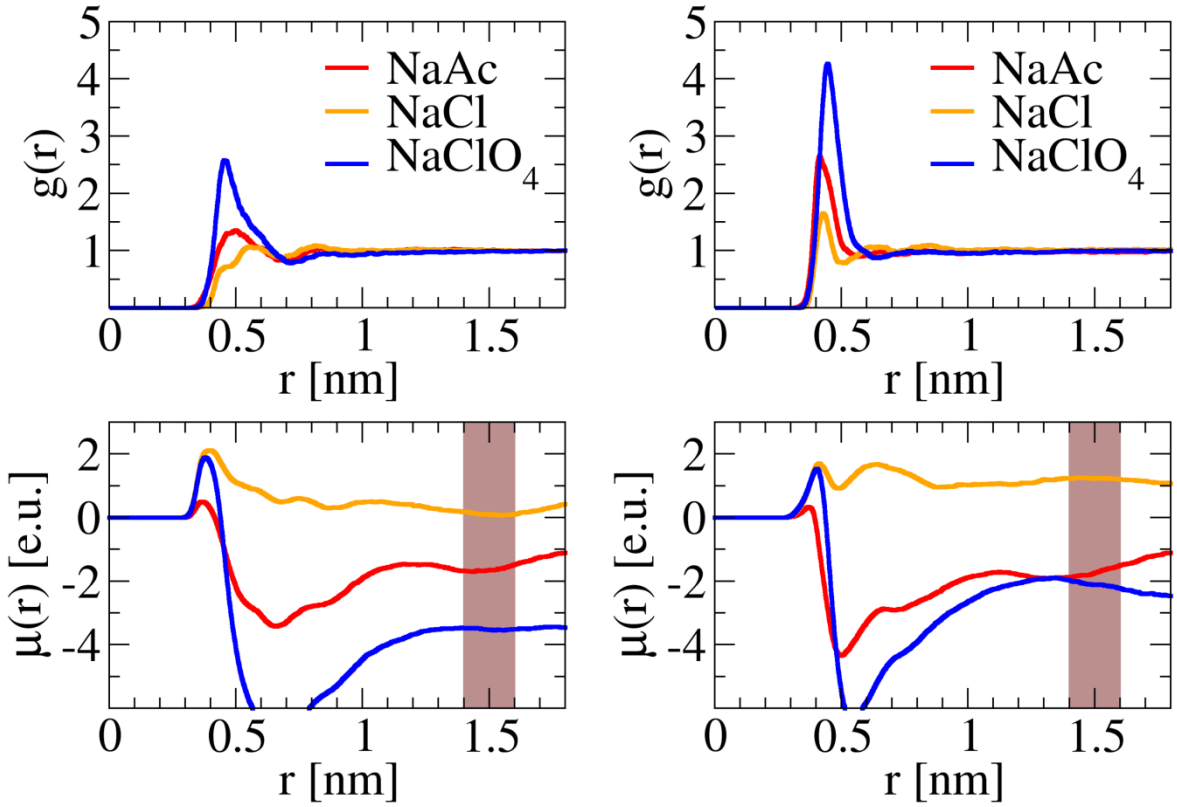

Figure 5: Structural properties of selected sodium salts (Ac^- - red, Cl^- – orange, ClO_4^- – blue, Na^+ - green) previously shown in Figures 3, and 4 are here presented in terms of spatial distribution functions. Cuts through 3D density map for two selected values are plotted around NMA (2nd column), and thiourea (3rd column). The water oxygen distribution (red) around solutes is shown in the last row for comparison. The contours are shown at 3.5x (opaque), and 1.8x (transparent) the bulk density value for anions; at 2.6x (opaque), and 1.8x (transparent) the bulk density value for sodium cation; and at 1.7x (opaque), and 1.4x (transparent) the bulk density value for water oxygen. Structures of anions are provided in the first column for the reader's convenience.

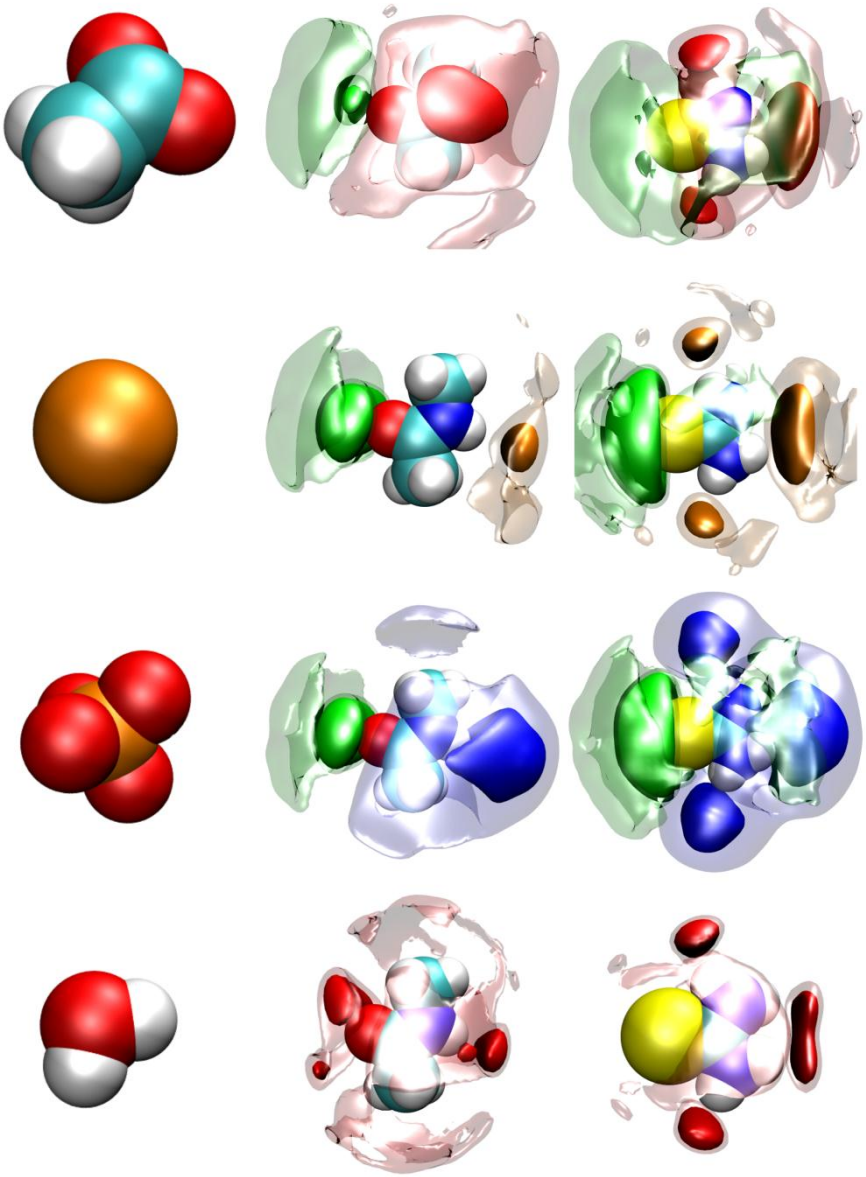

Supplementary Information

Electroneutrality condition and consequences on $g_{S\text{-}ion}(r)$ for cation and ions

In section 2.5.2 we have shown that structure of solution in terms of radial distribution functions has direct consequences on the absolute electrophoretic mobility of solute, S. Although locally the g(r) for cation (*c*) and anion (*a*) are independent, on sufficiently large scales (*R*>1nm) their integrals (number of ions N_{ion}) are coupled due to electroneutrality condition, $0 = \sum_{i=X^+,Y^-} z_i N_i$.

In terms of g(r) this can be expressed as:

$$(4)\quad z_c N_c^{S,ex}(\varrho_c) = 4\pi z_c \varrho_c \int_0^R (g_{S-c}(r) - 1) r^2 \mathrm{d}r = 4\pi z_a \varrho_a \int_0^R (g_{S-a}(r) - 1) r^2 \mathrm{d}r = z_a N_a^{S,ex}(\varrho_a)$$

Table S1: Solvent accessible surface area of investigated molecules, and its decomposition to the polar and nonpolar (methyl) groups. The polar contribution is in addition split to partially negative/positive parts (H-bond acceptors/donors region).

ASA [Å^2]	DMSO	NMA	thiourea
nonpolar	163	183	33
polar	59 (47/11)	54 (38/16)	170 (116/54)
total	222	237	203

Table S2: For MD simulation of all acetate salts investigated here we used the parameterization from reference [27]. As Cs^+ was not included in the original set of alkali metals, we chose the following parameters of Lennard-Jones 12-6 potential, which seem to be reasonable extension of the original set.

	σ_{Cs}	ε_{Cs}
Cs^+	4.2 Å	0.2 kJ/mol

Table S3: Relative electrophoretic mobility of NMA with respect to thiourea as measured in sodium salts mixed with sodium acetate/acetic acid buffer (v/v : 4/1, same ionic strength). Slopes $d\Delta\mu/dc$ are determined based on best linear fits of experimental data in Figure 2.

Salt/buffer	$d\Delta\mu_{NaX/NaAc}^{NMA,TUR}/dc_{NaX}$ $[10^{-9}\cdot m^2\cdot V^{-1}\cdot s^{-1}\cdot mol^{-1}\cdot l]$
Na_2SO_4/NaAc	4.0
NaAc	0.0
NaF/NaAc	1.6
NaCl/NaAc	1.2
$NaClO_4$/NaAc	-0.9
CH_3SO_3Na/NaAc	0.8
NaI/NaAc	---
NaSCN/NaAc	---

Table S4: Piecewise contributions of individual ions to absolute electrophoretic mobilities as calculated via equation 3 based on ion-solute radial distribution function are summarized. The absolute mobilities caused by salt (cation+anion contribution to mobilization) are included. The relative mobility (NMA-thiourea, or NMA-DMSO) are also calculated. Please note that the excluded volume itself (ions cannot penetrate inside of the solute) gives rise from 3.25 e.u./M (for 3Å sphere), up to 5 e.u./M (for 4Å sphere). The excluded volume effect naturally vanishes for the overall salt effect (the cation-anion difference).

	$\Delta\mu_{salt}^{NMA\text{-}marker}$		NMA			DMSO			Thiourea		
	vs. **TUR**	vs. **DMSO**	μ_{Na+}^{NMA}	μ_{X-}^{NMA}	μ_{salt}^{NMA}	μ_{Na+}^{DMSO}	μ_{X-}^{DMSO}	μ_{salt}^{DMSO}	μ_{Na+}^{TUR}	μ_{X-}^{TUR}	μ_{salt}^{TUR}
Na_2SO_4	**0.1**	**-1.2**	-6.8	6.0	**-0.8**	-6.4	6.8	**0.4**	2.5	-3.4	**-0.9**
NaAc	**0.1**	**-0.6**	-6.5	4.9	**-1.6**	-8.3	7.3	**-1.0**	-4.6	2.9	**-1.7**
NaF	**1.3**	**0.6**	-10.8	12.0	**1.2**	-12.7	13.3	**0.6**	-4.0	3.9	**-0.1**
NaCl	**-1.1**	**0.1**	-6.4	6.5	**0.1**	-4.6	4.6	**0.0**	-2.3	3.5	**1.2**
NaI	**-2.9**	**0.2**	-4.3	3.7	**-0.6**	-5.4	4.6	**-0.8**	-2.7	5.1	**2.4**
$NaClO_4$	**-1.4**	**-1.4**	-6.7	3.2	**-3.5**	-4.4	2.2	**-2.2**	-0.5	-1.6	**-2.1**
NaSCN	**-0.6**	**0.8**	-3.3	2.1	**-1.2**	-4.2	2.2	**-2.0**	-2.0	1.4	**-0.6**
CH_3SO_3Na	**1.2**	**1.1**	-6.6	6.6	**0.0**	-6.6	5.5	**-1.1**	-1.7	0.6	**-1.1**

	$\Delta\mu_{salt}^{NMA\text{-}marker}$		NMA			DMSO			Thiourea		
	vs. **TUR**	vs. **DMSO**	μ_{X+}^{NMA}	μ_{Ac-}^{NMA}	μ_{salt}^{NMA}	μ_{X+}^{DMSO}	μ_{Ac-}^{DMSO}	μ_{salt}^{DMSO}	μ_{X+}^{TUR}	μ_{Ac-}^{TUR}	μ_{salt}^{TUR}
LiAc	**1.5**	**-1.0**	-5.9	5.6	**-0.3**	-4.3	4.9	**0.7**	-2.6	0.8	**-1.8**
NaAc	**0.1**	**-0.6**	-6.5	4.9	**-1.6**	-8.3	7.3	**-1.0**	-4.6	2.9	**-1.7**
KAc	**-1.0**	**0.3**	-7.3	5.7	**-1.6**	-7.3	5.4	**-1.9**	-1.2	0.6	**-0.6**
CsAc	**-1.0**	**-0.9**	-9.4	7.0	**-2.4**	-6.5	5.0	**-1.5**	-1.3	-0.1	**-1.4**

Figure S1: Structural properties of all investigated acetate salts are presented in terms of cation-solute radial distribution functions (top panel). Thereafter calculated electrophoretic mobilities (according to equation 3) are presented in bottom panel. Results for NMA are present on the left, for thiourea in the middle and for DMSO on the right. The mobility coefficients as extracted from the brown region are summarized in Table S4, the NMA and thiourea mobility differences are presented in Table 2. Colors of cations and acetate salt are the following: Li^+/LiAc - black, Na^+/NaAc – green, K^+/KAc – blue, Cs^+/CsAc – pink.

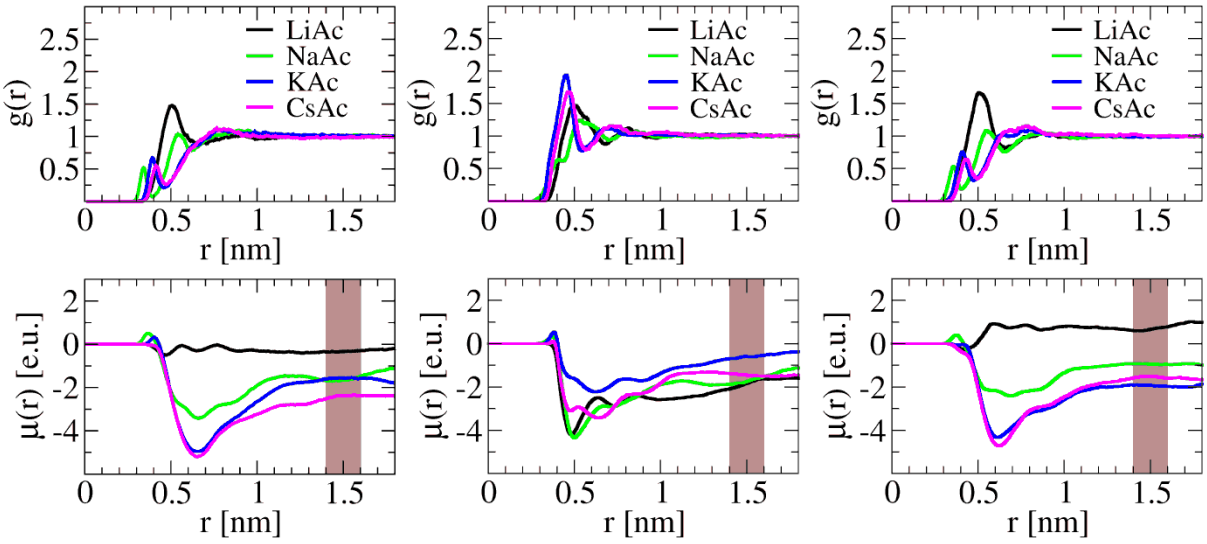

Figure S2: Structural properties of all investigated sodium salts are present in terms of anion-solute radial distribution functions (top panel). Thereafter calculated electrophoretic mobilities (according to equation 3) are presented in bottom panel. Results for NMA are present on the left, for thiourea in the middle and for DMSO on the right. The mobility coefficients as extracted from the brown region are summarized in Table S4, the NMA and thiourea mobility differences are presented in Table 3.

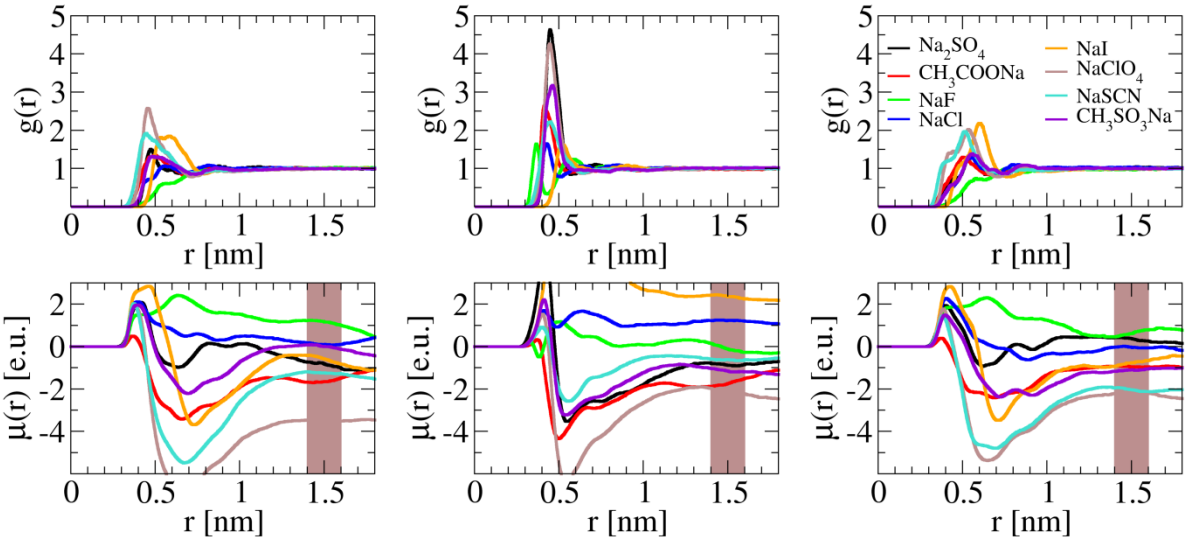

Figure S3: Structural properties of all investigated sodium salts (anion is always red, Na^+ - green) previously shown in Figure S2 are here presented in terms of spatial distribution functions. Cuts through 3D density map for two selected values are visualized around NMA (2nd column), DMSO (3rd column), and thiourea (4th column). The water oxygen distribution (red) around solutes is shown in the first row. The contours are shown at 3.5x (opaque), and 1.8x (transparent) the bulk density value for anions (red); at 2.6x (opaque), and 1.8x (transparent) the bulk density value for sodium cation (green); and at 1.7x (opaque), and 1.4x (transparent) the bulk density value for water oxygen. Structures of anions are provided in the first column for the reader's convenience.

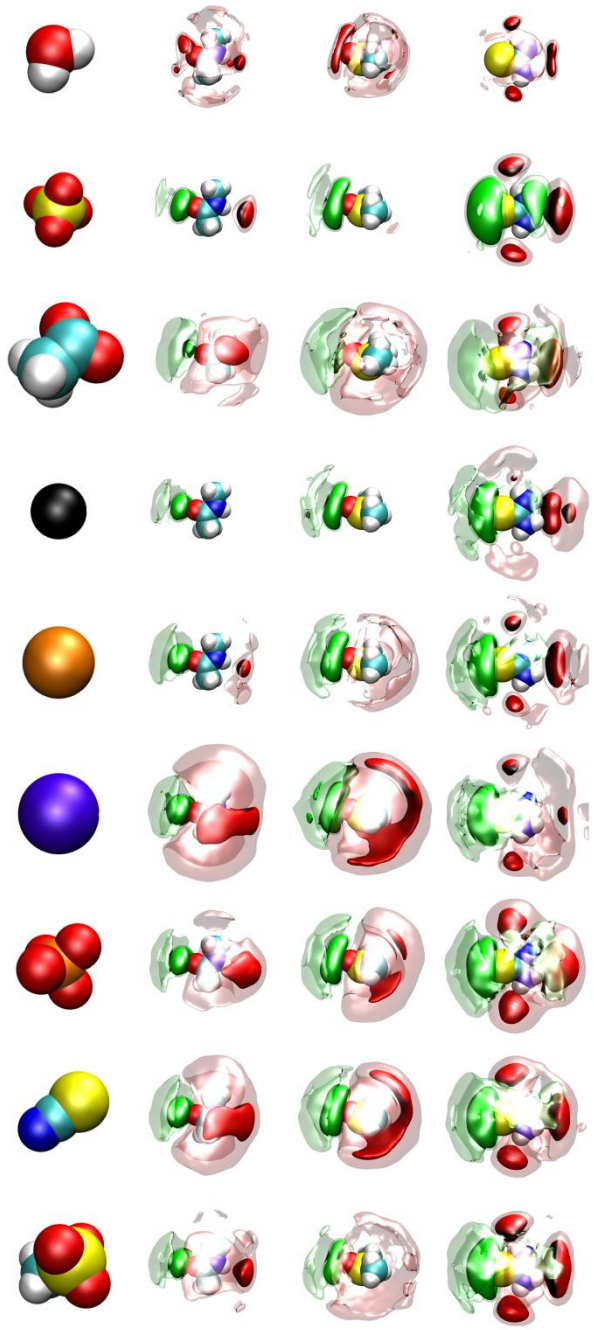

Figure S4: Structural properties of all investigated acetate salts (Ac^- - red, Li^+ - black, Na^+ - green, K^+ - blue, Cs^+ - pink) previously shown in Figure S1 are here presented in terms of spatial distribution functions. Cuts through 3D density map for two selected values are visualized around NMA (2nd column), DMSO (3rd column), and thiourea (4th column). The water oxygen distribution (red) around solutes is provided in Figure 5 and S3. The contours are shown at 3.5x (opaque), and 1.8x (transparent) the bulk density value for anion; at 2.6x (opaque), and 1.8x (transparent) the bulk density value for cations. Rough relative sizes of cations are included in the first column for the reader's convenience.

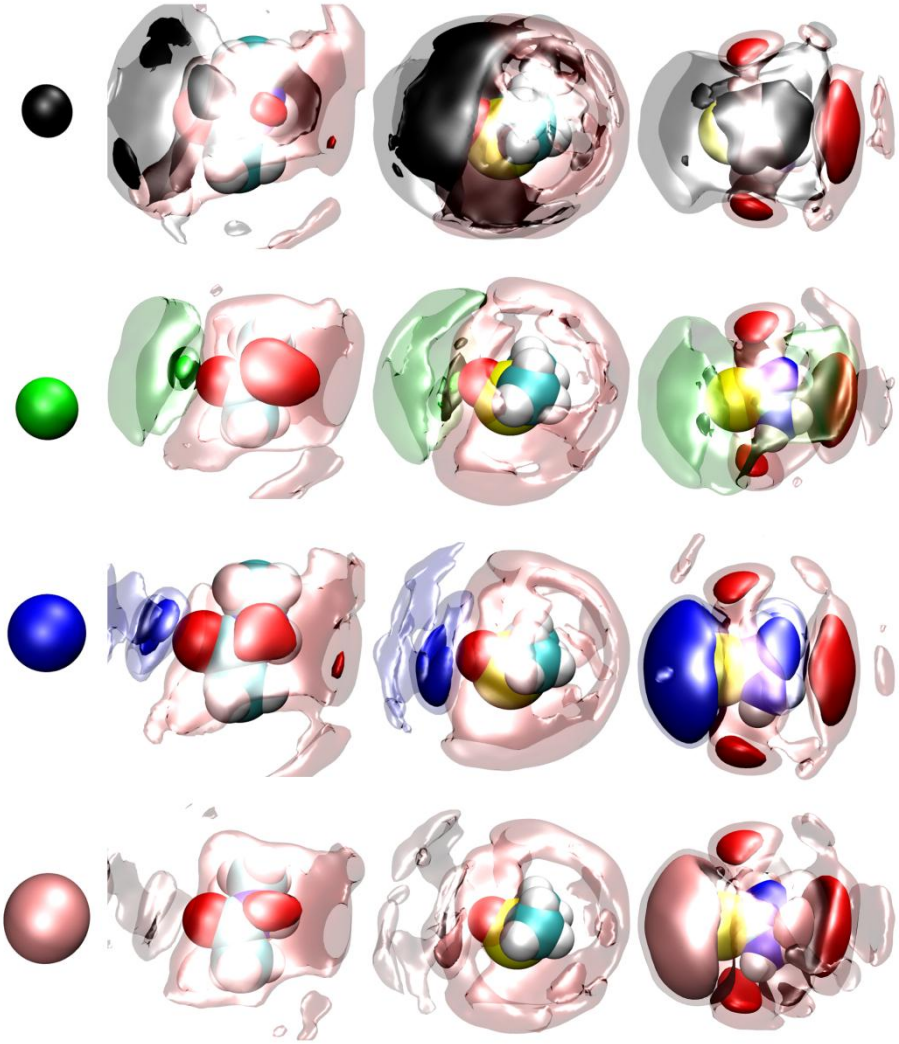

Figure S5: Effect of cation (Li^+ - black, Na^+ – green, K^+ – blue, and Cs^+ - pink) on the acetate-solute radial distribution function (so called counterion effect). Counterion effects on NMA are presented on the left, on thiourea in the middle and on DMSO on the right.

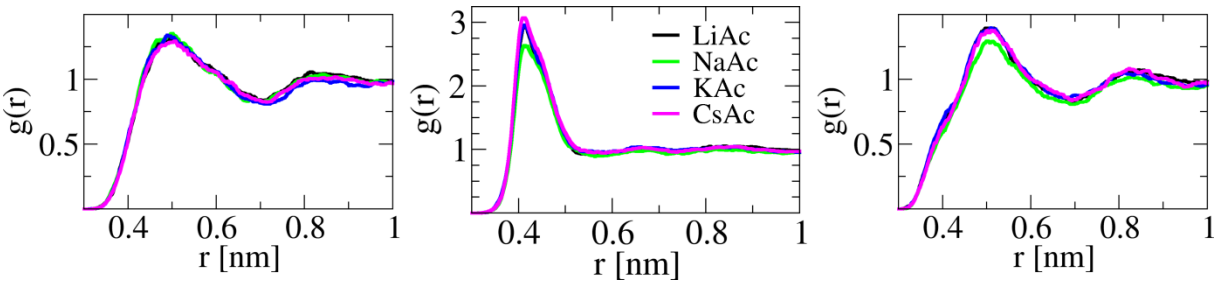

Figure S6: Effect of anion (SO_4^{2-} - black … $CH_3SO_3^-$ - pink, see the legend in the first figure) on the sodium-solute radial distribution function (so called counterion effect). Counterion effects on NMA are presented on the left, on thiourea in the middle and on DMSO on the right. Note that for sodium sulphate and sodium acetate different parameters for sodium cation are employed. For all the other salts we used the exactly same sodium parameter [27].

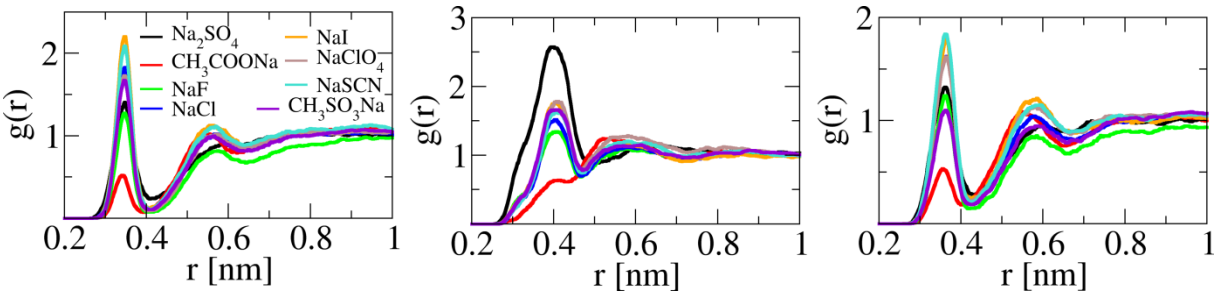

TOC graphics

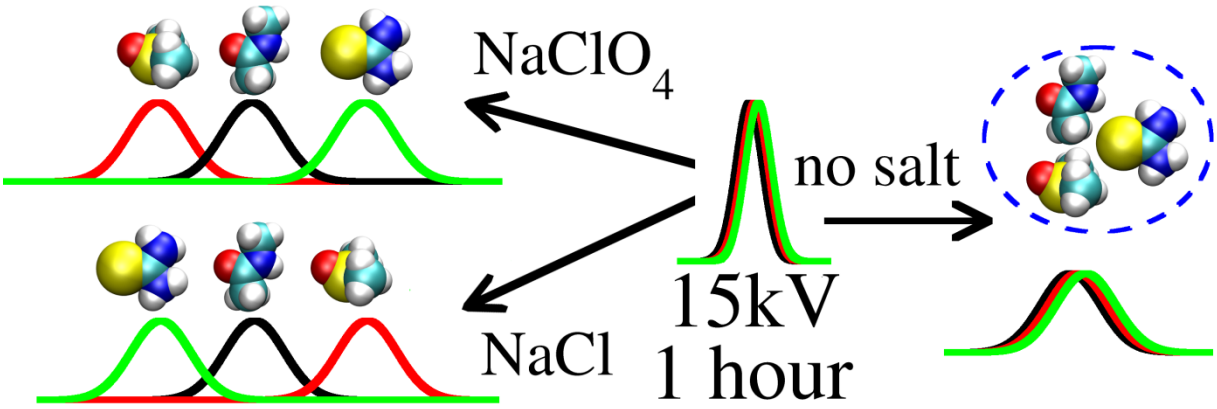

References:

[27] Hess, B., van der Vegt, N. F. A., *Proceedings of the National Academy of Sciences* 2009, *106*, 13296-13300.